2011-09

Photoelectrochemical, photophysical and morphological studies of electrostatic layer-by-layer thin films based on poly(p-phenylenevinylene) and single-walled carbon nanotubes

Photochemical and Photobiological Sciences,Cambridge : Royal Society of Chemistry - RSC, v. 10, n. 11, p. 1766-1772, Sept. 2011
http://www.producao.usp.br/handle/BDPI/50030

Photochemical & Photobiological Sciences

An international journal

www.rsc.org/pps

Volume 10 | Number 11 | November 2011 | Pages 1717–1838

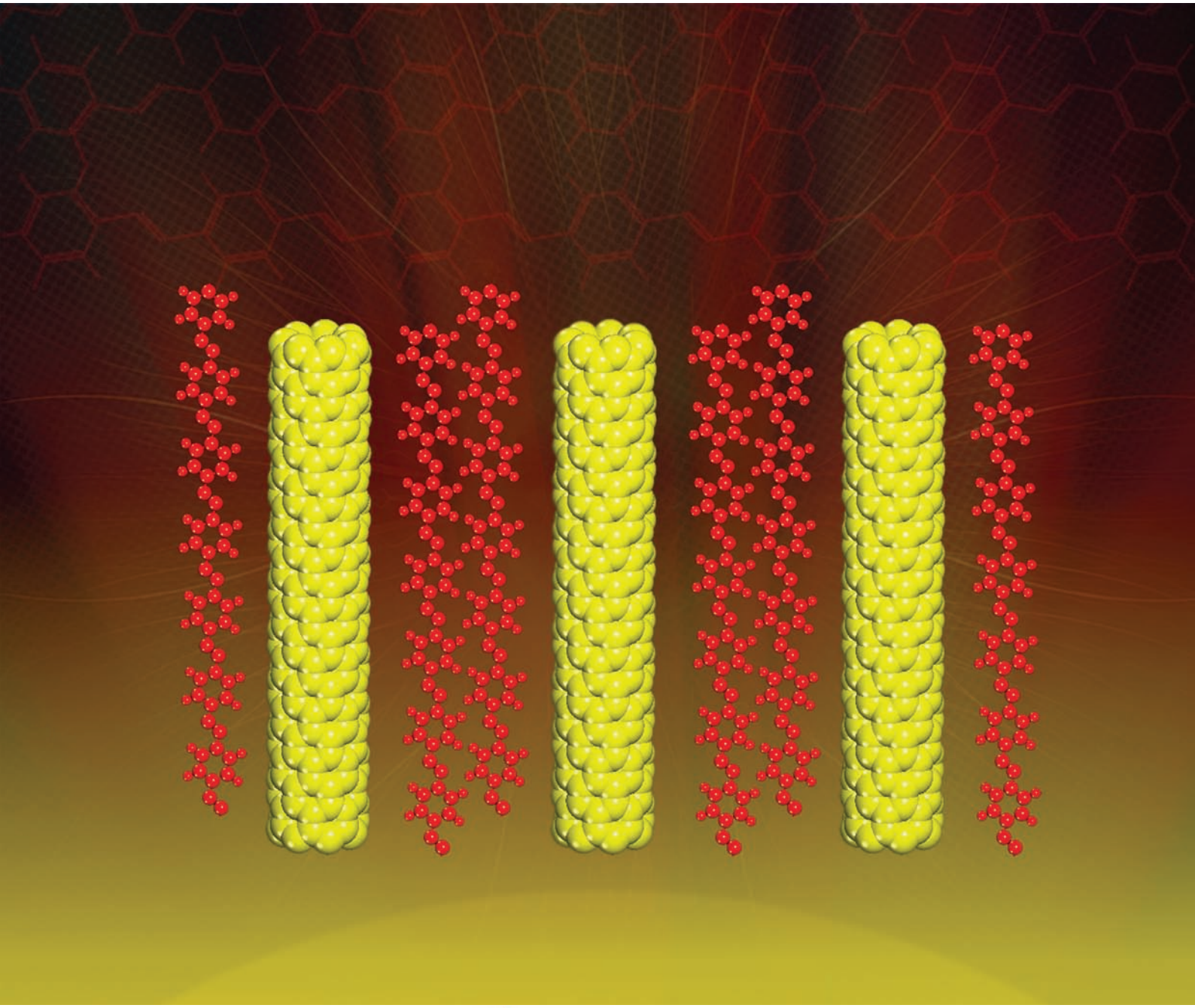

ISSN 1474-905X

RSC Publishing

1474-905X(2011)10:11;1-1

Photochemical & Photobiological Sciences

Dynamic Article Links

Cite this: *Photochem. Photobiol. Sci.*, 2011, **10**, 1766

www.rsc.org/pps

PAPER

Photoelectrochemical, photophysical and morphological studies of electrostatic layer-by-layer thin films based on poly(*p*-phenylenevinylene) and single-walled carbon nanotubes

L. C. P. Almeida,[a] V. Zucolotto,[b] R. A. Domingues,[a] T. D. Z. Atvars[a] and A. F. Nogueira*[a]

Received 13th July 2011, Accepted 27th July 2011
DOI: 10.1039/c1pp05221g

The preparation of multilayer films based on poly(*p*-phenylenevinylene) (PPV) and carboxylic-functionalized single-walled carbon nanotubes (SWNT-COOH) by electrostatic interaction using the layer-by-layer (LbL) deposition method is reported herein. The multilayer build-up, monitored by UV-Vis and photoluminescence (PL) spectroscopies, displayed a linear behavior with the number of PPV and SWNT-COOH layers deposited that undergo deviation and spectral changes for thicker films. Film morphology was evaluated by AFM and epifluorescence microscopies showing remarkable changes after incorporation of SWNT-COOH layers. Films without SWNT show roughness and present dispersed grains; films with SWNT-COOH layers are flatter and some carbon nanotube bundles can be visualized. The photoinduced charge transfer from the conducting polymer to SWNT-COOH was analyzed by PL quenching either by the decrease of the emission intensity or by the presence of dark domains in the epifluorescence micrographs. Photoelectrochemical characterization was performed under white light and the films containing SWNT-COOH displayed photocurrent values between 2.0 μA cm^{-2} and 7.5 μA cm^{-2}, as the amount of these materials increases in the film. No photocurrent was observed for the film without carbon nanotubes. Photocurrent generation was enhanced and became more stable when an intermediate layer of PEDOT:PSS was interposed between the active layer and the ITO electrode, indicating an improvement in hole transfer to the contacts. Our results indicate that these multilayer films are promising candidates as active layers for organic photovoltaic cells.

Introduction

Composites based on conducting polymers and single-walled carbon nanotubes (SWNT) have been the subject of intense studies due to their potential application in technological areas such as sensors,[1] light emitting diodes[2] and solar energy conversion,[3] just to name a few. Conducting polymers are one example of materials frequently used as an active media for electroluminescent and photovoltaic devices because of their good electrical and optical properties that can be easily tuned according to their chemical structure.[4–6] Furthermore, conducting polymers offer several possibilities of processability for small and large areas, on rigid or flexible substrates.[7] Different wet-processing techniques such as spin-coating, dip-coating, ink-jet printing and screen printing at room temperature can be employed, which are very attractive approaches for producing less expensive, flexible and large area films with a good control of thickness.[7]

Carbon nanotubes are also a very appealing material for electronic devices due to their electron affinity, imposed by the large extended π conjugation, high charge mobility,[8] high surface area and good thermal and chemical stabilities.[9] Furthermore, carbon nanotubes may be prepared with a wide range of direct gaps (optical and electrochemical) matching the solar spectrum[10] and show a notable photoresponse upon absorption from ultraviolet to infrared spectral regions.[11]

Among the different types of deposition techniques, the layer-by-layer self-assembling technique (LbL) has drawn great attention as a simple and versatile approach for preparing thin composites films.[12,13]

In general, the build-up of LbL films with charged species involves deposition by electrostatic interactions between species in solution with opposite charges forming a new layer to compensate the underlying one of a different charge. When this process takes place without deep penetration of the layers, the mass and the thickness of the film increases linearly with the number of bilayers. On the other hand, if during the deposition there is a deep interpenetration between the layers, the growing follows an

[a]*Institute of Chemistry, University of Campinas – UNICAMP, P.O. Box 6154, 13083-970, Campinas, SP, Brazil. E-mail: anaflavia@iqm.unicamp.br; Fax: +55 19 35213023; Tel: +55 19 3521302*
[b]*Physics Institute of São Carlos, USP, P.O. Box 369, 13560-970, São Carlos, SP, Brazil*

exponential profile with the number of bilayers.[14,15] Furthermore, LbL films may be very smooth for thicknesses corresponding to the deposition of 20–30 bilayers (these numbers depend on the materials), however grains can be observed for thicker films.[16] Therefore, regardless of the growth regime, good control of the thickness as well as of the morphology can be obtained during LbL film formation.

Rubner *et al.*[17] prepared LbL thin films based on PPV and fullerene derivatives and reported an efficient polymer luminescence quenching produced by photoinduced electron transfer (a very fast process) between the MEH-PPV and C_{60}. In another work,[18] they also fabricated photovoltaic devices with a heterojunction consisting of 20 bilayers of PPV/poly(acrylic acid) and 60 bilayers of C_{60}/poly(allyl amine hydrochloride), which exhibited photovoltages of 0.7–0.8 V and efficiency of 10^{-2}–10^{-3}%.

More detailed photoelectrochemical studies have been applied to LbL films aiming at a better understanding of the charge transfer processes that occur between donor and acceptor materials.[19] Guldi *et al.*[20] evaluated the charge transfer process from photoactive ITO electrodes to a LbL film composed of a fullerene-porphyrin (H_2P) dyad. For this system, they concluded that the injection of electrons into the ITO conduction band occurs basically in two steps: directly from the photochemically generated $H_2P^{\bullet+}$–$C_{60}^{\bullet-}$ radical pair and indirectly *via* electron transport mediated through suitable electron carriers (*i.e.*, O_2 and methyl viologen).

Zotti *et al.*,[21–23] using hybrid LbL films of semiconductor nanocrystals (CdS, CdSe and PbSe) and organic semiconductor polymeric materials (polythiophene derivatives) showed the influence of different parameters on the charge transfer processes. They concluded that these hybrid structures can be easily produced from solution and that they are promising candidates for hybrid organic-inorganic solar cells. Sgobba *et al.*[24] assembled LbL donor/acceptor photoelectrodes of positively and negatively charged polythiophenes and single-walled carbon nanotubes, reproducing a bulk heterojunction active layer. These photoelectrodes were tested in photoelectrochemical devices, providing monochromatic IPCE values of 8.2%. Thus, the possibility to strategically build a combination between donor and acceptor materials using LbL deposition techniques seems to be an interesting alternative to control more accurately film morphology and produce efficient photovoltaic devices.

In this work, we report the photoelectrochemistry, photophysical and morphological studies of LbL films based on poly(*p*-phenylenevinylene) (PPV) and carboxylic acid functionalized single-walled carbon nanotubes (SWNT-COOH) *via* LbL deposition. Bilayer devices were formed by two blocks of multilayers, in which an electron-donating film (100 bilayers of PPV/DBS) deposited onto ITO electrodes was followed by deposition of an electron-accepting block comprised of $(PEI/SWNT\text{-}COOH)_m$ bilayers (where m = 3, 5 and 8), resulting in a final $[(PPV/DBS)_{100}|(PEI/SWNT\text{-}COOH)_m]$ architecture. Multilayer sorption and film growth were investigated upon collecting the electronic spectra of the films after deposition of each PPV/DBS bilayer. The photophysical properties of the luminescent LbL $(PPV/DBS)_{100}$ and of the $(PPV/DBS)_{100}|(PEI/SWNT\text{-}COOH)_m$ layers (m = 3, 5 and 8) are obtained from the PL data and the photoinduced electron transfer was analyzed using photocurrent generation measurements.

Experimental

Materials

Poly(xylylidenetetrahydrothiophenium chloride) (PTHT), branched poly(ethylenimine) (PEI, MW ~25 000), poly(3,4-ethylenedioxythiophene)-poly(styrenesulfonate) (PEDOT:PSS) (1.3 wt% dispersion in H_2O), ethylene glycol (EG, anhydrous, 99.8%), sodium dodecylbenzenesulfonate (DBS) and carboxylic acid functionalized single-walled carbon nanotubes (SWNT-COOH) were all purchased from Sigma–Aldrich and used without further purification (see Fig. 1 for chemical structures). The SWNT sample used is a mixture of metallic and semiconducting tubes.

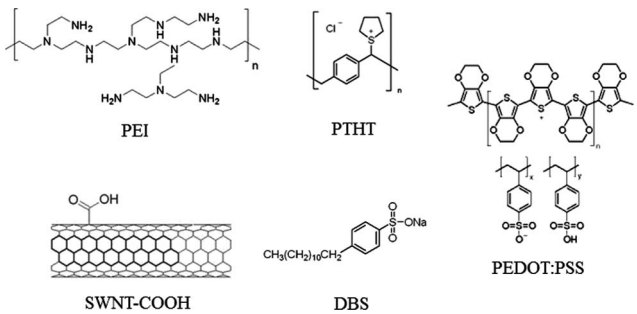

Fig. 1 Chemical structures of the materials used in the preparation of the LbL films used in this work.

Multilayer thin film assembly

The LbL multilayers were deposited onto optical (BK-7) and ITO-coated glass substrates. Cleaning of the optical glasses was achieved using a classical procedure. The substrates were previously dipped in detergent solution (1% w/w) under sonication for 10 min and then immersed for 30 min in a 1 : 1 mixture of concentrated H_2SO_4 and 30% H_2O_2 followed by extensive rinsing with ultrapure water obtained from a Milli-Q system from Millipore. The substrates were immersed in a 1 : 1 : 5 mixture of 25% NH_4OH, 30% H_2O_2 and ultrapure H_2O at 70 °C to add hydroxyl groups to their surfaces and then thoroughly rinsed with ultrapure water. The ITO-coated glasses were sequentially cleaned with commercial detergent solution (1 wt%), ultrapure water, acetone and ethanol using an ultrasonic bath (5 min for each treatment). Afterwards, the substrates were immersed in a 1 : 1 : 5 mixture of 25% NH_4OH, 30% H_2O_2 and ultrapure H_2O for 10 min to ensure that the surfaces were clean and abundant in hydroxyl groups. PTHT, PEI and DBS solutions were prepared at concentrations of 2.2×10^{-6}, 2.0×10^{-6} and 1.0×10^{-5} mol mL^{-1}, respectively in deionized water (polyelectrolyte concentrations are with respect to the repeating units). The aqueous SWNT-COOH dispersion was prepared at a concentration of 0.05 mg mL^{-1}, assisted by an application of ultrasound during 30 min.

The LBL deposition process of the vinylenephenylene-DBS bilayers were conducted automatically by a programmable dipping machine (Haubenteuer MG-1100) and started with the deposition of donor layers comprising PTHT and DBS, by alternate dipping into each solution for 1 min. After each immersion the substrate was dipped in ultrapure water for 1 min.

This procedure was repeated until the desired number of (PTHT/DBS) bilayers was achieved. After assembly, the films were heated at 110 °C for 2 h under vacuum. This procedure converts PTHT into PPV as represented in the Scheme 1. In sequence, acceptor layers of SWNT-COOH and PEI were also deposited onto the (PPV/DBS) blocks. Initially, the substrate containing the (PPV/DBS) block was immersed alternately in PEI solution and in the SWNT-COOH dispersion for 1 min, each step followed by the same washing procedure mentioned before. The final architectures obtained were $(PPV/DBS)_n$ and $[(PPV/DBS)_n|(PEI/SWNT\text{-}COOH)_m]$, where n varies from 1 to 100 and m varies from 1 to 8.

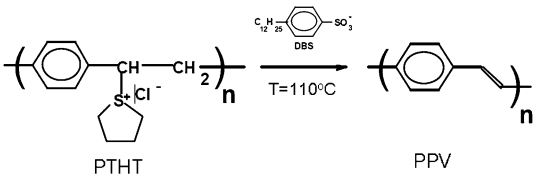

Scheme 1 Thermal conversion process of the cationic precursor PTHT into PPV polymer.[26]

For optical and morphological characterization, composite films were deposited onto optical glasses, and for the photoelectrochemical measurements they were deposited onto ITO and ITO containing a thin hole-transporting layer (HTL) of PEDOT:PSS (ITO/PEDOT:PSS). The HTL was prepared from an aqueous dispersion of PEDOT:PSS (1.3 wt%, 5 g) mixed with EG (13 mg) as described elsewhere.[25] The mixed solution was spin-coated at 400 rpm for 10 s and then 3000 rpm for 99 s and thermally annealed at 70 °C for 14 h in air and at 140 °C for 1 h under vacuum to give an insoluble film of PEDOT:PSS.

Methods

The UV-Vis absorption spectra of the multilayer thin films were measured with a Hewlett–Packard HP-8453 spectrophotometer. Steady state photoluminescence (PL) spectra were obtained using an ISS-PC1 spectrofluorimeter with a photon counting detection system in front-face illumination. The samples were excited at 420 nm and the fluorescence emission was collected in the range of 450–700 nm.

Epifluorescence micrographs (EFM) were recorded in a Leica DM IRB inverted fluorescence microscope employing objectives with optical magnification values of 25 ×. A 100 W Hg arc lamp was employed with the excitation wavelength range selected as 330–380 nm by optical filters. The emission image was separated from the excitation beam by a dichroic mirror ($\lambda_{exc} > 410$ nm). Atomic force microscopy (AFM) images were obtained with a Digital Nanoscope III in the tapping mode.

The photoelectrochemical (PEC) experiments were performed with an Eco Chimie-Autolab PGSTAT 12 potentiostat. Chronoamperometric measurements were performed using a three electrode configuration cell (Ag/AgCl as reference electrode, ITO (or ITO/PEDOT:PSS) covered films as working electrode and a platinum plate (1.0 × 2.0 cm^2) as counter electrode) at room temperature. The multilayer films were irradiated though the ITO side (substrate/electrode interface, SE). 0.1 mol L^{-1} solution of KCl in water saturated with O2 was employed as electrolyte. The PEC cell was placed in an optical bench consisting of an OrielXe(Hg) 250 W lamp coupled to an AM 1.5 filter (Oriel), collimating lenses and a water filter (Oriel). The light intensity was calibrated with an optical power meter; model 1830-C (Newport) to *ca.* 100 mW cm^{-2}, but no corrections were made for reflections and transmission losses.

Results and discussion

Optical characterization of the multilayered films

Once deposited, the PTHT and DBS layers were allowed to react thermally producing bilayers of PPV/DBS. The optical properties of the LbL films were investigated by UV–Vis absorption and PL spectroscopies. Fig. 2a depicts the changes in the absorption spectra of PPV/DBS multilayer films with different numbers of layers deposited. The broad absorption band extending from 350 to *ca.* 500 nm is attributed to π–π* absorption transitions between delocalized states coupled with the vibronic states of PPV chains.[26] Contribution to the broadening by chains with a distribution of molecular weights cannot be disregarded. The absorbance of the PPV π–π* at 400 nm increases linearly with the increase in number of bilayers deposited (inset of Fig. 2a) in agreement with the results

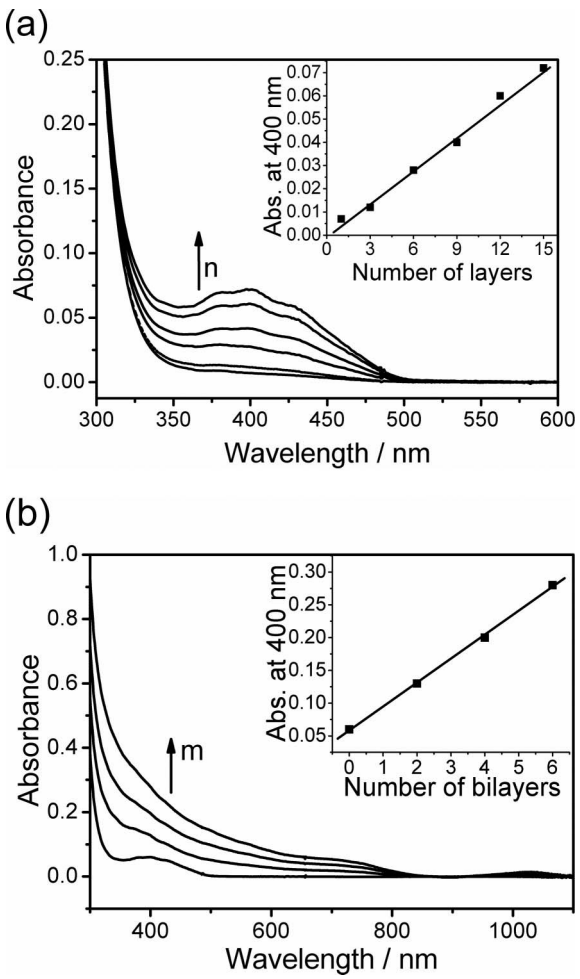

Fig. 2 (a) UV-Vis spectra of the $(PPV/DBS)_n$ films (n = 1, 3, 6, 9, 12 and 15) and (b) the $[(PPV/DBS)_{12}|(PEI/SWNT\text{-}COOH)_m]$ films, where m is the number (PEI/SWNT-COOH) bilayers equal to 2, 4 and 6.

observed by Marletta *et al.*[27] This behavior indicates that there is no interpenetration between the layers during the deposition, at least up to 15 layers.[15,16]

The deposition of 2, 4 and 6 (PEI/SWNT-COOH) bilayers on a $(PPV/DBS)_{12}$ block, shown in Fig. 2b, also presented a linear behavior of the absorbance *versus* number of layers. This suggests that there is no interpenetration between the (PEI/SWNT-COOH) bilayers or between them and the $(PPV/DBS)_{12}$ block. The absorption spectra presented three characteristic regions: a longer scattering curve, characteristic of the semiconductor behavior from UV to the visible; absorption bands of the $(PPV/DBS)_{12}$ (350–500 nm); absorption bands (600–800 nm and around 1000 nm) attributed to the interband transitions of semiconductor SWNT (S2) and metallic SWNT (M1).[28]

We did not go further with the numbers of (PEI/SWNT-COOH) bilayers since the percolation thresholds of SWNT/polymer nanocomposites are reached at a very low amount of carbon nanotubes.[29] Several studies on organic solar cells using carbon nanotubes in the active film, including ours, suggest a maximum of 1–5% (w/w) of this material.[3,30–33]

PPV/DBS films were also monitored by PL spectroscopy (Fig. 3a) and, based on the emission intensity, their growth is essentially linear at least up to 15 bilayers. This is in agreement with UV-Vis spectroscopy results (Fig. 2a). All PPV/DBS emission spectra exhibited the same peak position and a well-resolved vibronic structure, with the 0-0 phonon band at 492 nm. We observed gradual enhancement in the PL intensity of the (PPV/DBS) films by increasing the number of bilayers, *i.e.*, increasing the amount of the luminescent material that is often cited as the reason for increasing PL intensity.[34] The well-defined vibronic structure and the practically constant ratio between the vibronic intensities present in all spectra suggests that the PPV chains are emitting as isolated species and are not undergoing energy transfer processes to aggregates nor forming excimer or exciplex species. In addition, due to the higher intensity if the 0-0 band, inner filter effect is practically absent in this thinner films.

For photoelectrochemical characterization, it is important to achieve a good collection of the excitation light, thus, we needed to increase the thickness layer of the PPV block, even though the morphology will change from flat surface films to a film with grains. Thus, films of PPV/DBS with 100 bilayers were deposited. These films displayed a suitable absorbance for our proposal. Nevertheless, films with 100 bilayers show remarkable spectral changes, Fig. 3b. For this film, the absorption peak is broader and red-shifted, which is characteristic of aggregated species. The PL spectrum is also red-shifted with an emission maximum at 550 nm, which can be attributed to presence of aggregates. The strong decrease of the 0-0 phonon band at 492 nm may be attributed to several reasons: the energy transfer from the isolate forms to aggregates, the inner filter effect due to the greater thickness of these films and the resonant non-radiative energy transfer process due to the interlayer chain interpenetration in thicker films. At present we do not have enough data to select among them.

We also studied the PL spectra of the $(PPV/DBS)_{100}$ substrate with PEI/SWNT-COOH bilayers (from 3 to 8) (Fig. 4a). PL spectra showed that, as the number of bilayers containing SWNT deposited on $(PPV/DBS)_{100}$ increases, a decrease of the PPV photoluminescence intensity is observed, as indicated by the plot of the I_F/I_{F0} (550 nm) *versus* number of bilayers, where I_{F0} is the

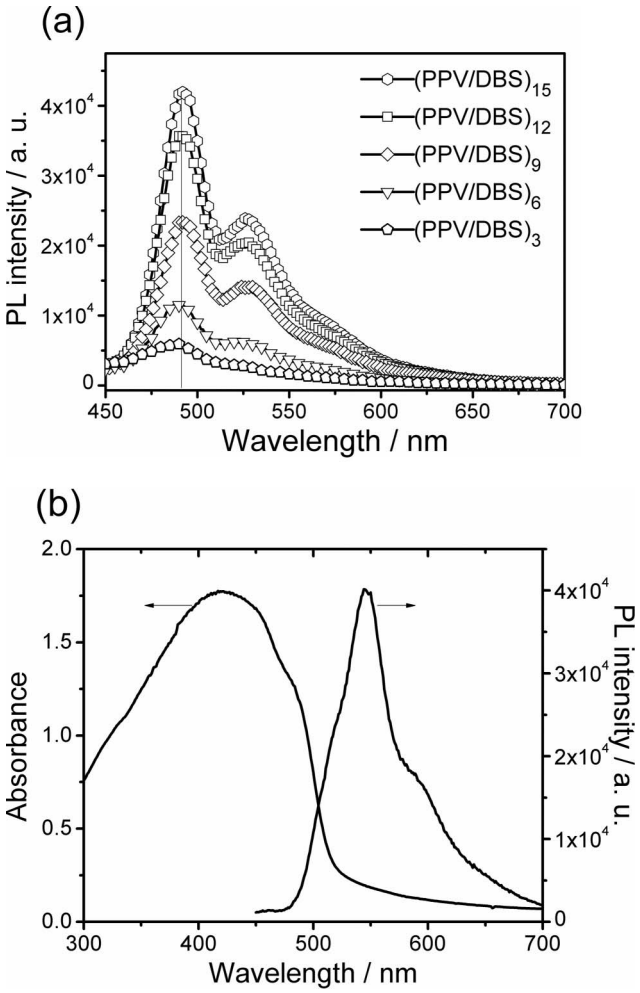

Fig. 3 (a) Photoluminescence spectra of the $(PPV/DBS)_n$ films excited at 420 nm, where n is the number of bilayers and (b) for the film containing 100 layers of PPV/DBS. The absorption spectrum of this film is also shown.

intensity at 550 nm of $(PPV/DBS)_{100}$ and I_F is intensity at 550 nm of $(PPV/DBS)_{100}$ in the presence of the $(PEI/SWNT-COOH)_m$ (Fig. 4b). Such behavior is not linear as expected for assemblies where chain interpenetration from one block towards the opposite charged block is occurring. We will reinforce this possibility in the next section, where film morphology data is discussed.

PL quenching after deposition of $(PEI/SWNT-COOH)_m$ layers over the PPV/DBS block can be a consequence of electron or energy transfer processes occurring at the interface between these materials. Because electron transfer is a short distance process,[35] there is a greater probability that it will be more efficient around the interface (heterojunction) between the $(PPV/DBS)_{100}$ and $(PEI/SWNT-COOH)_m$ blocks. This type of process involving conjugated polymers and fullerenes is well established in the literature.[36] Although electron transfer between $(PPV/DBS)_{100}$ and $(PEI/SWNT-COOH)_m$ is a quite plausible process, trivial energy transfer and resonant non-radiative processes involving PPV/DBS chain interpenetration cannot be discarded and it is probably responsible for the change of the emission profile, in particular for the relative decrease of the higher energy edge of the emission band.[34] Here we are not considering resonance energy transfer process by the Förster mechanism as playing a major role because

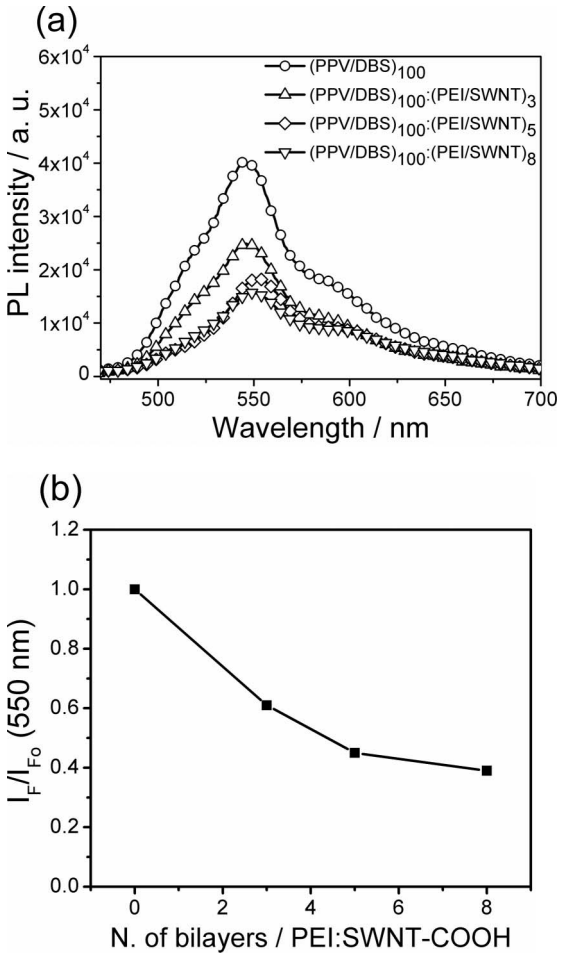

Fig. 4 (a) Photoluminescence spectra of the $[(PPV/DBS)_{100}|(PEI/SWNT\text{-}COOH)_m]$ films where m is equal to 3, 5 and 8, and (b) the respective percentage decrease of photoluminescence intensity measured (at λ_{max} = 550 nm) as function of number of PEI/SWNT-COOH layers.

the electron transfer process may play a major role between the PPV excited state and the PEI/SWNT-COOH.[37,38]

Morphology of the LbL films

The morphology of the $(PPV/DBS)_{100}$ block and for the di-block $[(PPV/DBS)_{100}|(PEI/SWNT\text{-}COOH)_m]$ (where m = 3, 5 and 8) were initially analyzed by epifluorescence microscopy (Fig. 5). For the block $(PPV/DBS)_{100}$ (Fig. 5a) we can see a bright yellow emission over the entire sample with spaced bright grains, as expected for thicker LbL films. After deposition of 3 bilayers of PEI/SWNT-COOH onto the $(PPV/DBS)_{100}$ block (Fig. 5b) some weaker emission is noted, and distributed over the entire sample. Again, bright grains are also noted, indicating that the $(PEI/SWNT\text{-}COOH)_3$ covered the grains of the $(PPV/DBS)_{100}$ but now some dark domains appeared from the SWNT-COOH nanotubes present in the (PEI/SWNT-COOH) bilayers. The relative contribution of these dark domains increases upon increasing the number of (PEI/SWNT-COOH) bilayers to 5 and 8, *i.e.*, upon increasing the carbon nanotube concentration, a more pronounced decrease in the PL intensity was observed (Fig. 5c and 5d). These dark domains are attributed to the SWNT-

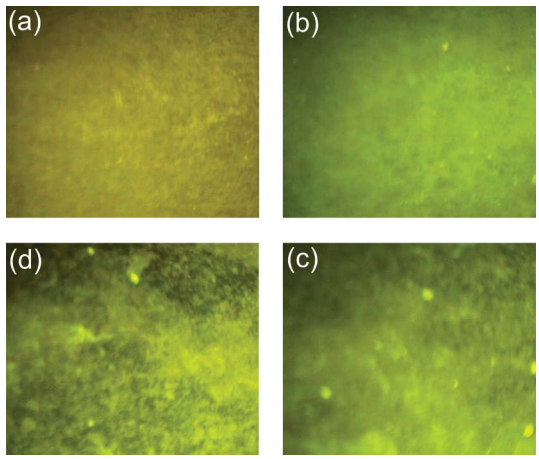

Fig. 5 Epifluorescence microscopy of (a) $(PPV/DBS)_{100}$, $(PPV/DBS)_{100}|(PEI/SWNT\text{-}COOH)_m$ with m = 3 (b), m = 5 (c) and m = 8 (d) LbL films deposited onto an optical glass substrates (scanned area of 50 × 50 μm²).

COOH which quench the emission of the $(PPV/DBS)_{100}$ block. This quenching mechanism has already been discussed and may be attributed to energy and/or electron transfer processes. It is important to clarify that we mean by "SWNT concentration" as the number of SWNT per unit area of the film.

The morphology of the LbL films were also investigated by tapping mode AFM images, for a scanned area of 5.0 × 5.0 μm². The image for the $(PPV/DBS)_{100}$ film (Fig. 6a) depicts an almost fully covered surface with high roughness factor (41.27 nm). It suggests the formation of a non-uniform coating, indicating that higher loadings of bi-layer deposition formed thicker and rougher films with the presence of grains, as indicated by epifluorescence microscopy. After the deposition of (PEI/SWNT-COOH) bilayers onto the (PPV/DBS) substrate, a clear modification in morphology can be observed. In samples with $(PEI/SWNT\text{-}COOH)_3$

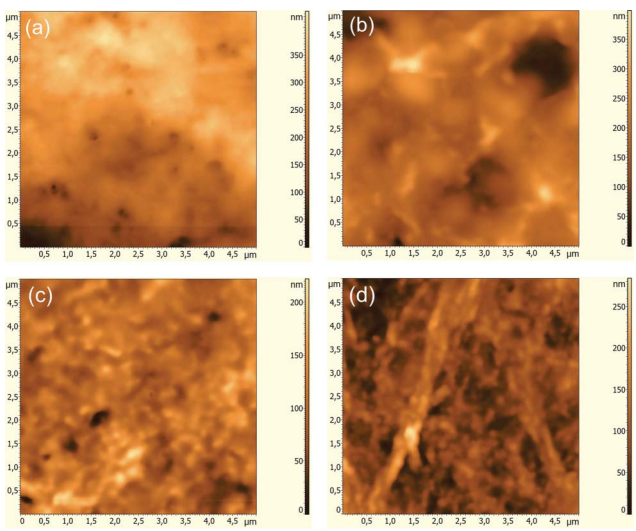

Fig. 6 AFM images of (a) $(PPV/DBS)_{100}$, (b) $(PPV/DBS)_{100}|(PEI/SWNT\text{-}COOH)_3$, (c) $(PPV/DBS)_{100}|(PEI/SWNT\text{-}COOH)_5$, (d) $(PPV/DBS)_{100}|(PEI/SWNT\text{-}COOH)_8$ LbL films deposited onto ITO—glass substrates (scanned area of 5.0 × 5.0 μm²).

(Fig. 6b) and (PEI/SWNT-COOH)$_5$ (Fig. 6c) the surface is still rougher, depicting RMS values of 41.83 and 41.03 nm, respectively. Furthermore, small grains are still observed for both samples. For the (PEI/SWNT-COOH)$_8$ block, thin bundles of SWNT were observed and appeared embedded within the polymer layers as can be seen in Fig. 6d. This block provided an efficient coverage of the rough (PPV/DBS)$_{100}$ film, changing the roughness factor from 41.27 nm to 19.25 nm. The agglomerates observed in Fig. 6b–d, related to the presence of polymer embedded-carbon nanotubes are in agreement with epifluorescence images (dark domains that quenched PPV emission), discussed previously.

Photoelectrochemical measurements

In order to evaluate the photoelectrochemical properties of the LbL films compromised of PPV-DBS and PPV-DBS/SWNT-COOH, these films were employed as working electrodes in a classical three-electrode cell. Chronoamperometric measurements were carried out (at 0 V bias) in an aqueous solution of KCl saturated with dioxygen which acts as electron transport mediator.

As depicted in Fig. 7, the film containing only PPV/DBS bilayers showed a small photoactivity, *i.e.*, a very low photocurrent (~nA) owing limited exciton dissociation and charge transport through the 100 bilayers. When layers of carbon nanotubes were deposited onto the PPV/DBS bilayers, appreciable values of photocurrent appeared immediately under illumination and dropped down under dark regimes. This indicates that the carbon nanotubes can act as dissociation centers for the excitons generated on the PPV chains, thus increasing the number of the charge carriers that reach the electrolyte interface. The cathodic photocurrent observed for all multilayer films indicate that the electron flux is towards the electrolyte, where dioxygen is responsible for shuttling the electrons to the Pt plate electrode. The difference on the shape of the time dependence curves after the first cycle for the films containing 5 and 8 layers of SWNT may be associated to a more limited transport in thick films.

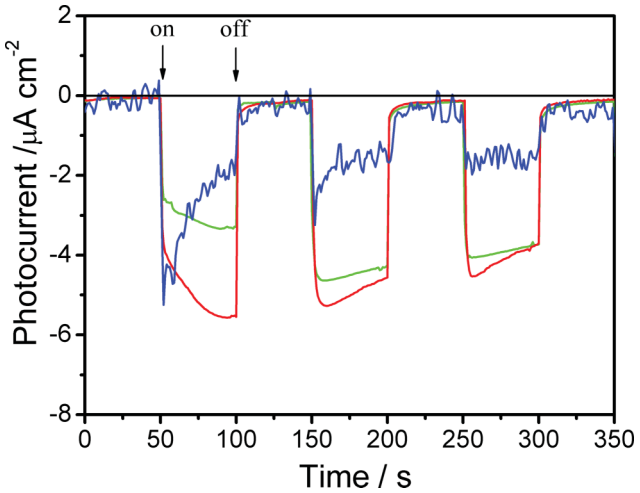

Fig. 7 Photocurrent generation from ITO electrodes bearing multilayer film (black) (PPV/DBS)$_{100}$, (blue) (PPV/DBS)$_{100}$|(PEI/SWNT-COOH)$_3$, (red) (PPV/DBS)$_{100}$|(PEI/SWNT-COOH)$_5$ and (green) (PPV/DBS)$_{100}$|(PEI/SWNT-COOH)$_8$ coverages under visible light irradiation (aqueous solution containing 0.1 mol L^{-1}KCl as supporting electrolyte saturated with O_2; no bias voltage was applied).

An enhancement in the photocurrent values was also verified by increasing the number of layers of carbon nanotubes, indicating that these carbon nanostructures are promising materials for exciton dissociation and charge transport. This observation was demonstrated by Strano and co-workers.[39]

Photocurrent generation can be related to the transfer of photogenerated electrons or holes on PPV to the carbon nanotubes, as suggested by the photoluminescence data presented. Liu *et al.*[40] demonstrated recently that single-walled carbon nanotubes are more effective in transporting holes than electrons, but this discussion is still under debate in the literature.

The evaluation of photocurrent generation in a photoelectrochemical cell is often a complex problem, since coexisting contributions such as charge transport inside the film and charge injection toward the electrode and/or the electrolyte can happen. As a consequence, the relative position of the HOMO/LUMO levels of the materials and the morphology of the film in contact with the electrolyte solution must certainly play an important role.

For the LbL film containing layers of PPV and carbon nanotubes, it can be assumed that the polymer/carbon nanotube interface allows the transfer of the photogenerated electrons or holes from PPV to SWNT carbon nanotubes, competing effectively with the deactivation processes in the conducting polymer, thus optimizing the charge transfer process. In our work, the AFM images show a continuous phase of PPV along the film, whilst only a small fraction of carbon nanotubes seems to be in close contact with the polymer. It means that the polymeric phase can offers significant pathways for charge transport (holes). On the other hand, the phase of carbon nanotube constituted of a few layers of agglomerated tubes (Fig. 6d) may present limited electron transport,[39] suggesting that it can be the bottleneck for photocurrent generation. In light of this, the morphology and the level of dispersion of the SWNT might play a relevant role in the total charge transport of the film.

Aiming to improve the photocurrent values and stability of the photoelectrochemical solar cells, a hole injection layer with good transport ability PEDOT:PSS[41–44] was introduced between the active layer and the ITO. Photocurrent responses of LbL film with and without the PEDOT:PSS hole injection layer are displayed in Fig. 8. Clearly, the films containing the PEDOT:PSS layer showed larger photocurrents and also improved photoelectrochemical stability in comparison to films without the PEDOT intermediate layer. This additional hole transport layer may be improving the hole transfer to ITO and then decreasing the electron-hole recombination, which can help to explain the enhancement in the photocurrent.

Conclusions

In this study we have described the preparation of multilayer films based on PPV/DBS and carboxylic functionalized SWNT-COOH by means of an electrostatic LbL assembly technique. The optical properties of the films were studied by UV-Vis spectroscopy that showed a linear behavior of the film growth at least up to 15 bilayers. PL results showed a considerable photoluminescence quenching for the LbL films containing layers of SWNT, indicating the occurrence of electron and/or energy transfer processes between the polymer and the nanotubes. Both epifluorescence microscopy and AFM images are in agreement

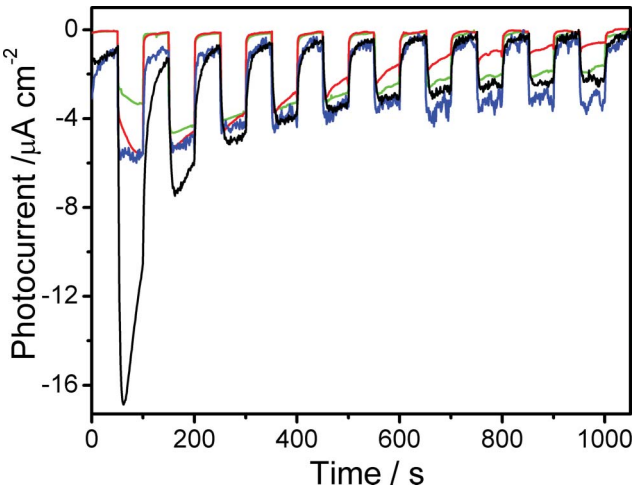

Fig. 8 Photocurrent generation from ITO electrodes bearing multilayer films (green) $(PPV/DBS)_{100}|(PEI/SWNT\text{-}COOH)_5$, (red) $(PPV/DBS)_{100}|(PEI/SWNT\text{-}COOH)_8$, (black) PEDOT:PSS|$(PPV/DBS)_{100}|(PEI/SWNT\text{-}COOH)_5$, (blue) PEDOT:PSS|$(PPV/DBS)_{100}|(PEI/SWNT\text{-}COOH)_8$ under visible light irradiation (*i.e.*, aqueous solution containing 0.1 mol L^{-1}KCl as supporting electrolyte saturated with O_2; no bias voltage was applied).

with the remarkable morphologic changes after incorporation of the carbon nanotubes onto the $(PPV/DBS)_{100}$ films. The LbL films displayed considerable photocurrent responses that are in agreement with the proposed charge transfer processes between polymer and nanotubes. A PEDOT:PSS intermediate layer played an important role by increasing photocurrent generation and photoelectrochemical stability of the films. We believe that the incorporation of the PEDOT layers enhances hole injection into the ITO contact.

Acknowledgements

The authors thank FAPESP (grant n° 08/53059-4 and 08/54017-3), CNPq and INEO-CNPq-Fapesp for the financial support and fellowships, the Centro de ComponentesSemicondutores (CCS) for providing AFM measurements and Prof. Carol Collins for English revision.

Notes and references

1 T. Zhang, M. B. Nix, B. Y. Yoo, M. A. Deshusses and N. V. Myung, *Electroanalysis*, 2006, **18**, 1153.
2 H. S. Woo, R. Czerw, S. Webstera, D. L. Carroll, J. W. Park and J. H. Lee, *Synth. Met.*, 2001, **116**, 369.
3 E. Kymakis and G. A. J. Amaratunga, *Appl. Phys. Lett.*, 2002, **80**, 112.
4 J. Peet, A. J. Heeger and G. C. Bazan, *Acc. Chem. Res.*, 2009, **42**, 1700.
5 Y. J. Cheng, S. H. Yang and C. S. Hsu, *Chem. Rev.*, 2009, **109**, 5868.
6 P. A. Sullivan and L. R. Dalton, *Acc. Chem. Res.*, 2010, **43**, 10.
7 A. C. Arias, J. D. MacKenzie, I. McCulloch, J. Rivnay and A. Salleo, *Chem. Rev.*, 2010, **110**, 3.
8 M. S. Fuhrer, B. M. Kim, T. Du1rkop and T. Brintlinger, *Nano Lett.*, 2002, **2**, 755.
9 M. Cinke, J. Li, B. Chen, A. Cassell, L. Delzeit, J. Han and M. Meyyappan, *Chem. Phys. Lett.*, 2002, **365**, 69.
10 M. J. O'Connell, S. M. Bachilo, C. B. Huffman, V. C. Moore, M. S. Strano, E. H. Haroz, K. L. Rialon, P. J. Boul, W. H. Noon, C. Kittrell, J. Ma, R. H. Hauge, R. B. Weisman and R. E. Smalley, *Science*, 2002, **297**, 593.
11 M. Freitag, Y. Martin, J. A. Misewich, R. Martel and P. Avouris, *Nano Lett.*, 2003, **3**, 1067.
12 G. Decher, *Science*, 1997, **277**, 1232.
13 G. Decher and J. B. Schlenoff, *Multilayer Thin Films: Sequential Assembly of Nanocomposite Materials*, Wiley-VCH, Weinheim, 2003.
14 P. Lavalle, C. Picart, J. Mutterer, C. Gergely, H. Reiss, J. C. Voegel, B. Senger and P. Schaaf, *J. Phys. Chem. B*, 2004, **108**, 635.
15 N. Hoda and R. G. Larson, *J. Phys. Chem. B*, 2009, **113**, 4232.
16 J. Seo, J. L. Lutkenhaus, J. Kim, P. T. Hammond and K. Char, *Macromolecules*, 2007, **40**, 4028.
17 M. Ferreira, M. F. Rubner and B. R. Hsieh, *MRS Symp. Proc.*, 1994, **328**, 119.
18 H. Mattoussi, M. F. Rubner, F. Zhou, J. Kumar, S. K. Tripathy and L. Y. Chiang, *Appl. Phys. Lett.*, 2000, **77**, 1540.
19 M. J. L. Santos, E. M. Girotto and A. F. Nogueira, *Thin Solid Films*, 2006, **515**, 2644.
20 D. M. Guldi, F. Pellarini, M. Prato, C. C. Granito and L. Troisi, *Nano Lett.*, 2002, **2**, 965.
21 G. Zotti, B. Vercelli, A. Berlin, P. T. K. Chin and U. Giovanella, *Chem. Mater.*, 2009, **21**, 2258.
22 G. Zotti, B. Vercelli, A. Berlin, M. Pasini, T. L. Nelson, R. D. McCullough and T. Virgili, *Chem. Mater.*, 2010, **22**, 1521.
23 B. Vercelli, G. Zotti, A. Berlin and M. Natali, *Chem. Mater.*, 2010, **22**, 2001.
24 V. Sgobba, A. Troeger, R. Cagnoli, A. Mateo-Alonso, M. Prato, F. Parenti, A. Mucci, L. Schenetti and D. M. Guldi, *J. Mater. Chem.*, 2009, **19**, 4319.
25 H. Benten, M. Ogawa, H. Ohkita and S. Ito, *Adv. Funct. Mater.*, 2008, **18**, 1563.
26 A. Marletta, D. Gonçalves, O. N. Oliveira, Jr., R. M. Faria and F. E. G. Guimarães, *Macromolecules*, 2000, **33**, 5886.
27 A. Marletta, F. A. Castro, C. A. M. Borges, O. N. Oliveira, Jr., R. M. Faria and F. E. G. Guimarães, *Macromolecules*, 2002, **35**, 9105.
28 H. Kataura, Y. Kumazawa, Y. Maniwa, I. Umezu, S. Suzuki, Y. Ohtsuka and Y. Achiba, *Synth. Met.*, 1999, **103**, 2555.
29 M. Moniruzzaman and K. I. Winey, *Macromolecules*, 2006, **39**, 5194.
30 B. J. Landi, R. P. Raffaelle, S. L. Castro and S. G. Bailey, *Progr. Photovolt.: Res. Appl.*, 2005, **13**, 165.
31 A. F. Nogueira, B. S. Lomba, C. R. D. Correia, C. A. Furtado, P. Corio and I. A. Hümmelgen, *J. Phys. Chem. C*, 2007, **111**, 18431.
32 G. Conturbia, R. C. G. Vinhas, R. Landers, G. M. S. Valente, V. Baranauskas and A. F. Nogueira, *J. Nanosci. Nanotechnol.*, 2009, **9**, 5850.
33 R. L. Patyk, B. S. Lomba, A. F. Nogueira, C. A. Furtado, A. P. Santos, R. M. Q. Mello, L. Micaroni and I. A. Hümmelgen, *Phys. Status Solidi RRL*, 2007, **1**, R43.
34 J. R. Lakowicz, *Principles of Fluorescence Spectroscopy*, Springer, New York, 2006.
35 J. J. M Halls, K. Pichler, R. H. Friend, S. C. Moratti and A. B. Holmes, *Appl. Phys. Lett.*, 1996, **68**, 3120.
36 N. S. Sariciftci, L. Smilowitz, A. J. Heeger and F. Wudl, *Science*, 1992, **258**, 1474.
37 J. W. Baur, M. F. Rubner, J. R. Reynolds and S. Kim, *Langmuir*, 1999, **15**, 6460.
38 H. L. Wang, D. McBranch, S. Xu, B. Kraabel, V. Klimov, R. Helgeson and F. Wudl, *Chem. Phys. Lett.*, 1999, **315**, 173.
39 M. H. Ham, G. L. C. Paulus, C. Y. Lee, C. Song, K. Kalantar-zadeh, W. Choi, J. H. Han and M. S. Strano, *ACS Nano*, 2010, **4**, 6251.
40 L. Liu and G. Li, *Appl. Phys. Lett.*, 2010, **96**, 083302.
41 W. U. Huynh, J. J. Dittmer, N. Teclemariam, D. J. Milliron and A. P. Alivisatos, *Phys. Rev. B: Condens. Matter*, 2003, **67**, 115326.
42 A. Petrella, M. Tamborra, M. L. Curri, P. Cosma, M. Striccoli, P. D. Cozzoli and A. Agostiano, *J. Phys. Chem. B*, 2005, **109**, 1554.
43 A. Petrella, M. Tamborra, P. Cosma, M. L. Curri, M. Striccoli, R. Comparelli and A. Agostiano, *Thin Solid Films*, 2008, **516**, 5010.
44 M. Lefebre, Z. Qi, D. Rana and P. G. Pickup, *Chem. Mater.*, 1999, **11**, 262.

